

# STOICHIOMETRY CONTROL OF COMPOUND SEMICONDUCTOR CRYSTALS (Part one)

Jun-ichi Nishizawa<sup>1)</sup>, Yutaka Oyama<sup>2)</sup>

Effects of stoichiometry on various feature of III-V compounds are investigated. The application of the optimum vapor pressure of group V elements is shown to minimize the deviation from the stoichiometric composition. Temperature dependence of the optimum vapor pressure is also obtained from both the annealing and the liquid phase epitaxial (LPE) growth experiments. Vapor pressure technology is successfully applied to the bulk crystal growth. In view of the defect formation mechanism, role of the stable interstitial As atoms ( $I_{As}$ ) in GaAs is emphasized. From the recent photocapacitance results, it is also shown that the excess group V atoms is also important for the formation of stoichiometry-dependent deep levels in InP and AlGaAs crystals. Even in the research field of surface science, it is shown that the precise control of stoichiometric composition should be required. Mechanism of the stoichiometry control is discussed on the basis of the equality of chemical potentials and the change of saturating solubility in the liquidus phase as a function of the vapor pressure. Stoichiometry-control should be also important in the field of the superconducting ceramics.

## 1. INTRODUCTION

The most important factor to be controlled is the deviation from the stoichiometric composition in compound semiconductor crystals. From the investigation of iron-pyrite in 1951 [1], the annealing experiments of various III-V compound semiconductor crystals have been carried out under controlled vapor pressure of group V elements [2, 3]. It is shown that the nearly perfect crystals with stoichiometric composition are obtained under a specific vapor pressure, and that the temperature dependence of the optimum vapor pressure is also obtained.

In view of the defect formation mechanism, the role of interstitial As atoms ( $I_{As}$ ) in GaAs crystals was emphasized when GaAs was annealed under high As vapor pressure [4]. Arsenic vapor pressure dependence on the specific weight and the intensity of X-

---

<sup>1)</sup> Tohoku University, Katahira Aoba-ku 2-1-1, Sendai 980, Japan

<sup>2)</sup> Semiconductor Research Institute, Semiconductor Research Foundation, Kawauchi Aoba-ku, Sendai 980, Japan

ray anomalous transmission implies the existence of As interstitial atoms [5]. Our Rutherford backscattering spectroscopy (RBS) experiments [6] have also revealed the As interstitial atoms in As<sup>+</sup>-implanted GaAs and determined the stable interstitial sites in the deformed lattices. The RBS results on the stable interstitial sites are in good accordance with those of X-ray anomalous transmission measurements [5].

The PHCAP measurements [7] under constant capacitance condition have shown the stoichiometry dependent deep levels and clarified the As vapor pressure dependencies of the deep level densities. The formation energy of the defects was also obtained to be 1.16 eV [8]. This relates most closely to the interstitial atoms, rather than to the vacancy. Recently much attention has been devoted on the interstitial As atoms in GaAs as well as the anti-site defect, because the so-called EL2 level relates to the excess As composition of GaAs crystals. Indeed, the recent results of X-ray quasi-forbidden reflection [9] seems to show the existence of the arsenic interstitial atoms.

Vapor pressure control technology has been also applied on the fields of bulk crystal growth. It is shown that high purity GaAs crystals were obtained with controlled composition and very low dislocation density as low as 2000 cm<sup>-2</sup> can be achieved even in 4-inch diameter Czochralski (CZ) grown semi-insulating GaAs crystals. This enables the fabrication of the super-bright LEDs [10], including the pure-green LEDs without nitrogen doping in GaP [11]. The vapor pressure control during crystal growth, which enables the control of the stoichiometric composition, is applied extensively not only on the III-V compounds e.g. InP, but on II-VI compounds including ZnSe [12].

This should be also important in the research field of the superconducting ceramics.

In the present paper, the annealing effects of GaAs under arsenic vapor pressure is shown. The electrical, optical and crystallographic properties are improved under a specific arsenic vapor pressure as designated to be the  $P_{opt}$ . In view of the stoichiometry-dependent deep levels, PHCAP results of the annealed GaAs and InP crystals are shown. Diffusion phenomenon in GaAs is closely related with the stoichiometric composition. Experimental results on diffusion of Cd and amphoteric impurity Si in GaAs are shown. It is shown that the amphoteric behavior of group IV elements (Sn [13] and Si [14]) in GaAs is controlled by the application of vapor pressure during LPE growth. LPE growth of GaAs under the controlled arsenic vapor pressure is also shown. This seems to continue to the results of melt growth by Suzuki and Akai [15], and also to that by Parsey et al [16]. Similar results are also obtained in LPE GaP under controlled phosphorus vapor pressure. Vapor pressure control technology is also extended into the GaAs bulk crystal melt growth. Crystal quality is shown as a function of the arsenic vapor pressure. In view of the non-stoichiometric defect formation mechanisms, the PHCAP and the RBS results are shown in combination with the results of crystal specific weight and X-ray anomalous transmission intensity measurements. The important role of arsenic interstitial atoms in GaAs is emphasized. In view of the surface stoichiometry and precise control of stoichiometric

composition during vapor phase epitaxial growth, experimental results of the molecular layer epitaxy (MLE) of GaAs is described. Importance of surface stoichiometry is also emphasized in the research field of surface science. Finally, theoretical consideration is also shown by taking into account the deviation from the stoichiometric composition.

## 2. ANNEALING OF GaAs UNDER CONTROLLED ARSENIC VAPOR PRESSURE

Annealing experiments were performed at 900 - 1100 °C for 67h under various As vapor pressure. Samples used were (100) oriented horizontal Bridgman (HB) grown GaAs with different impurity density. Defect density introduced by annealing reaches its saturating value after 67 h-annealing. Fig. 1 shows the schematic drawing

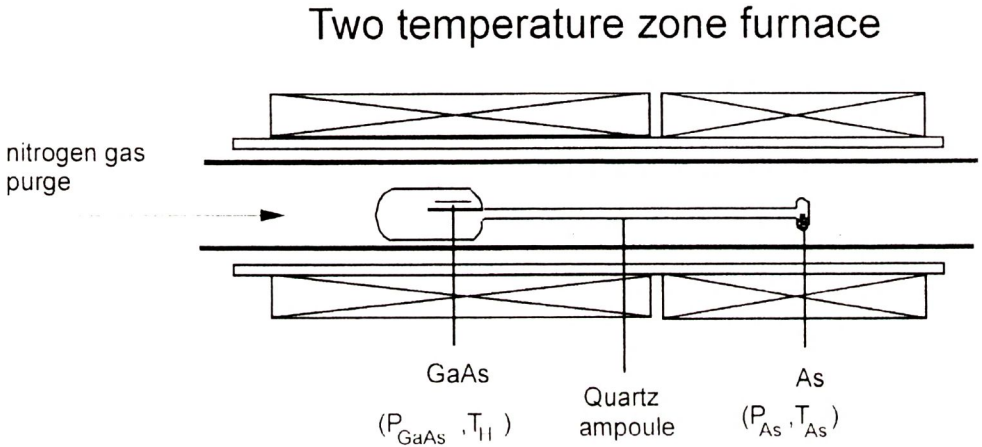


**Fig. 1.** Schematic drawing of the heat treatment equipment under controlled As vapor pressure of the annealing equipment under As vapor pressure. As vapor pressure applied on GaAs crystals was obtained as

$$P_{GaAs} = P_{As} \times (T_{GaAs} / T_{As})^{1/2} \quad (1)$$

where  $P_{As}$  is the equilibrium As vapor pressure determined from the temperature of arsenic metal ( $T_{As}$ ),  $T_{GaAs}$  is the temperature of GaAs crystals. Equilibrium As vapor pressure was obtained by Honig [17]. After annealing, samples were cooled rapidly by putting them into the water in order to prevent the effect of slow-cooling. X-ray and etching inspection cannot reveal slip lines even after rapid cooling.

Fig. 2 shows the change of acceptor density induced by annealing as a function

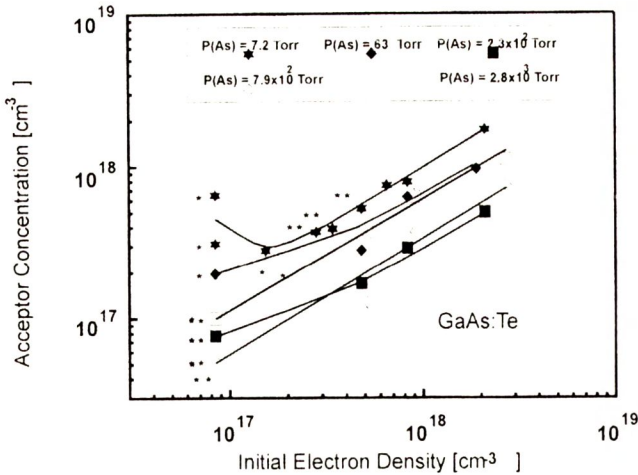


**Fig. 2.** Change of acceptor density induced by annealing as a function of the initial electron density in Te-doped

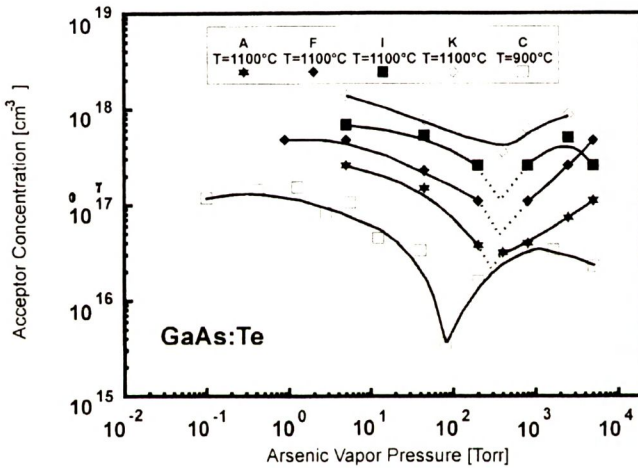


**Fig. 3.** As vapor pressure dependence of the acceptor density of Te-doped GaAs. Annealing was performed at 900 - 1100°C for 67h.

ned in Zn-doped GaAs crystals. Therefore, the  $P_{As,opt}$  is independent on the impurity concentration and dopant species. Almost the same results were also obtained in annealing experiments of GaP and optimum phosphorous pressure ( $P_{P,opt}$ ) was shown to improve the crystal quality. However, in case of GaP, lattice constant shows its maximum value under a specific phosphorus vapor pressure.

Consequently, optimum vapor pressures were obtained as a function of annealing

of the initial electron density in Te-doped GaAs after annealing. Acceptor density is almost equal to the initial electron density. This shows that the acceptor-type defects to both the deviation from stoichiometric composition and the dopant impurity Te and is the first finding of DX mixed level phenomena. Fig. 3 and Fig. 4 show the As vapor pressure dependencies of the acceptor density and of the lattice constant respectively. Lattice constant was measured by using X-ray double crystal diffraction with (004) symmetrical configuration. Various marks in the figures denote the data obtained from different crystals with different electron density. Acceptor density shows minimum under a specific As vapor pressure ( $P_{As,opt}$ ). Under almost the same As vapor pressure, lattice constant also shows its minimum value. It seems that the nearly perfect crystals with stoichiometric composition could be obtained under the  $P_{As,opt}$ . Almost the same results were obtained

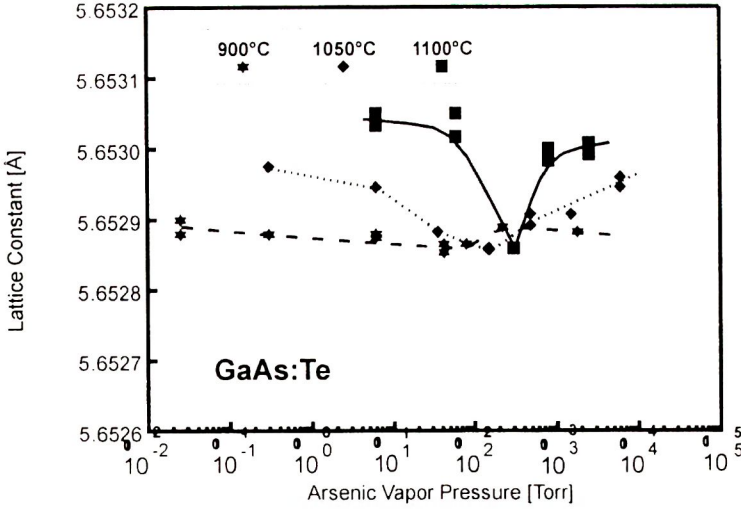


**Fig. 4.** As vapor pressure dependence of the lattice constant of Te-doped GaAs. Lattice constant was measured by the X-ray double crystal diffractometry analysis.

temperature for GaAs and GaP respectively as

$$P_{\text{GaAs,opt}} = 2.6 \times 10^6 \exp[-1.05 \text{ eV} / (kT)] \quad (2)$$

$$P_{\text{GaP,opt}} = 4.67 \times 10^6 \exp[-1.01 \text{ eV} / (kT)] \quad (3)$$

In order to investigate the deep levels in annealed GaAs crystals, the PHCAP measurements [18] were carried out under constant capacitance conditions [19]. The PHCAP method enables the precise determination of the level density and the activation energy because ionization by monochromatic light irradiation at fixed very low temperature were used. Contrary to the conventional PHCAP method, depletion layer thickness is kept to be constant regardless of the change of ion density by light irradiation.

In order to obtain accurate level density and level position, fully-neutralized deep levels should be ionized at each wavelength. One method to achieve such condition is application of forward bias injection in the dark before each photo-excitation. In *n*-type GaAs bulk crystals, the so-called photoquenching phenomenon [20] is observed in a specific wavelength region of about 1.0 -1.5eV below about 110 K. Therefore, both the maximum and the asymptotic to the saturation ion density were obtained at each wavelength.

Fig. 5 shows the PHCAP spectra of the intentionally-undoped GaAs ( $n=4 \times 10^{16} \text{ cm}^{-3}$ ) grown by HB method before annealing [21]. In the figure, (a) and (b) show the maximum ( $N_{\text{max}}$ ) and the asymptotic ion density ( $N_{\text{asym}}$ ) respectively, (c) represents the ion density ( $N_{\text{dark}}$ ) in the dark after forward bias injection.  $N_{\text{dark}}$  corresponds to the ion density in the dark before photoexcitation. Almost constant value of  $N_{\text{dark}}$

verifies the photo-excitation of fully-neutralized deep levels at each wavelength. Fig. 6 shows the PHCAP spectrum obtained from the subtraction of  $N_{\text{asym}}$  from  $N_{\text{max}}$ . This shows the deionized level density spectrum.

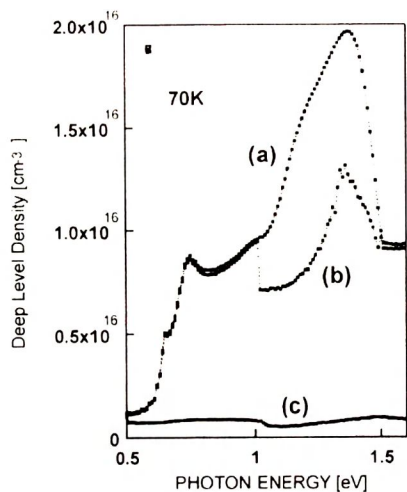


**Fig. 5.** Ion density PHCAP spectra of the intentional y-undoped GaAs ( $n = 4 \times 10^{16} \text{ cm}^{-3}$ ) grown by HB method before annealing: (a) and (b) show the maximum ( $N_{\text{max}}$ ) and the asymptotic ion density ( $N_{\text{asym}}$ ) respectively, (c) represents the ion density ( $N_{\text{dark}}$ ) in the dark after forward bias injection.

As shown in Fig.5, two kinds of deep donors were clearly revealed at 0.65 and 0.72 eV below the conduction band. The deionized level density spectrum shows clear two peaks at 1.25 and 1.41 eV respectively. 1.25 and 1.41 eV deep levels are quite different ones with different recovery temperature and ionized levels. Fig. 7 shows the PHCAP maximum ion density spectra of intentionally- undoped GaAs crystals prepared by annealing under various As vapor pressure. Fig. 8 shows the As vapor pressure dependencies of the  $E_c - 0.72$  eV level density. It is noticed that the  $E_c - 0.65$  eV level vanishes after annealing perhaps due to its thermal instability. However,  $E_c - 0.65$  eV level is stable in more strained crystals and the level density increases monotonically with increase of As vapor pressure. Level density of  $E_c - 0.72$  eV donor and the 1.25eV deionized level increases monotonically with increasing As vapor pressure. These deep levels are detected commonly in various GaAs bulk crystals with different do-

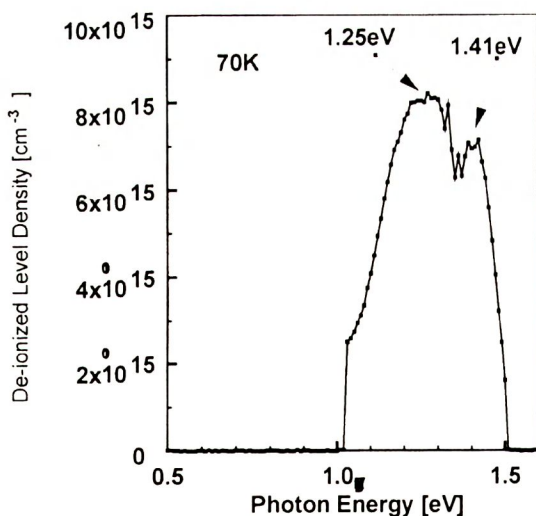


**Fig. 6.** Deionized level density PHCAP spectrum obtained from the subtraction of  $N_{\text{asym}}$  from  $N_{\text{max}}$ .

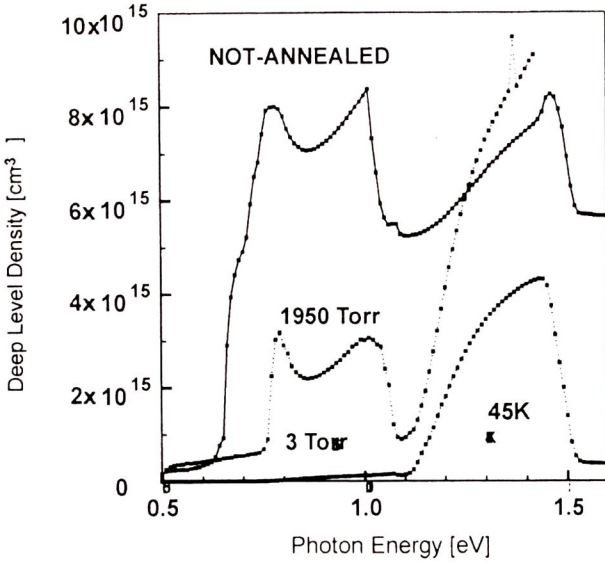


**Fig. 7.** PHCAP maximum ion density ( $N_{max}$ ) spectra of intentionally-undoped GaAs crystals prepared by annealing under various As vapor pressure. Annealing was performed at 900 °C for 67 h.

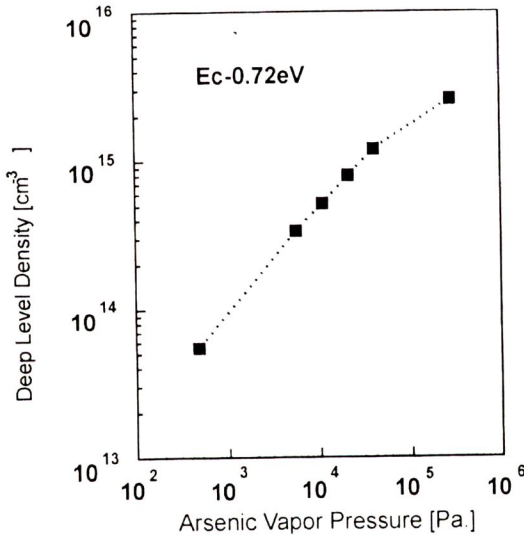


**Fig. 8.** As vapor pressure dependencies of the  $E_c - 0.72$  eV level density in intentionally-undoped GaAs ( $n = 4 \times 10^{16} \text{ cm}^{-3}$ ) grown by HB method. Annealing was performed at 900 °C for 67 h.

part impurity and conductivity type [22]. Monotonical increase of level density indicates that these deep levels closely relate with the excess As composition of GaAs crystal. From the spectral correspondence among the PHCAP, DLTS and deep level PL [23] at 2.1 K, it is shown that the  $E_c - 0.65$  and 0.72 eV level exhibit larger difference between optical and thermal activation energy compared with that of so-called the EL2 level. Whereas both our finding  $E_c - 0.72$  eV level and the so-called EL2 level are closely related with the excess arsenic composition of GaAs crystals, these are quite different from each other. They show different optical excitation energies and amount of Frank-Condon shift ( $d_{FC}$ ).

The PHCAP method also revealed the As-vacancy related deep levels in heavily Te-doped GaAs prepared by annealing under As vapor pressure [24]. Fig. 9 shows the As vapor pressure dependencies of the 0.62 and 0.87 eV +  $E_v$  level density, which were measured after 1.44 eV -monochromatic light irradiation at each wavelength to

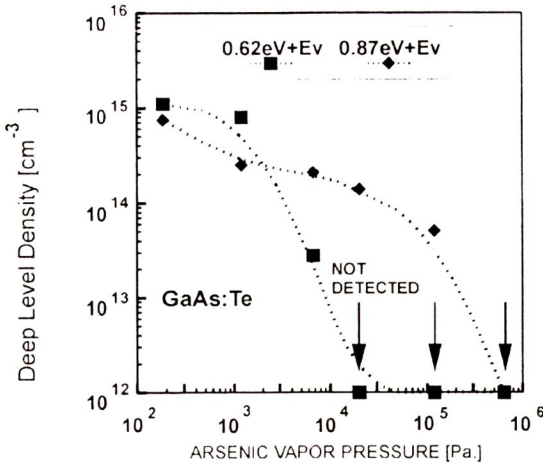


**Fig.9.** As vapor pressure dependencies of the 0.62 and 0.87 eV+ $E_v$  level density in heavily Te-doped GaAs ( $n = 7.4 \times 10^{17} \text{ cm}^{-3}$ ) prepared by annealing under As vapor pressure. PHCAF measurements were performed after 1.44 eV -monochromatic light irradiation at each wavelength to empty the deep levels.

empty the deep levels. The level density decreases monotonically with increasing As vapor pressure. These deep levels could be also detected in vacuum- annealed samples (500 °C for 50 h) but not be detected in the virgin samples. This confirms the close relation between these deep levels and the As vacancies.

The precise PHCAF measurements at 20 K revealed the stoichiometry-dependent deep levels at around  $E_c - 0.48 \text{ eV}$  in Te-doped horizontal gradient freeze (HGF) grown GaAs prepared by annealing under As vapor pressure. Level density decreases monotonically with increasing As vapor pressure.  $E_c - 0.48 \text{ eV}$  level was detected in Te-doped GaAs, but not be observed in intentionally-undoped nor Si doped GaAs crystals. Therefore, this should relate with at least the dopant impurity Te and the As vacancies.  $E_c - 0.72 \text{ eV}$  deep donor was also detected in the same samples, and the As vapor pressure dependence of the level density is almost the same as that in intentionally-undoped HB GaAs crystals. This suggests that the  $E_c - 0.72 \text{ eV}$  level is originated from the excess As atom-related intrinsic defects but not from some impurities.

### 3. LIQUID PHASE EPITAXIAL GROWTH BY THE TEMPERATURE DIFFERENCE METHOD UNDER CONTROLLED VAPOR PRESSURE (TDM-CVP)

Vapor pressure control technique was successfully applied to the LPE growth, and this enables to supply epitaxial layers with good crystal quality. Fig. 10 shows the schematic drawing of the LPE apparatus by TDM-CVP. Contrary to the conventional slow cooling method, crystal growth proceeds at a fixed substrate temperature with time. Temperature difference at the upper and lower part of the solution was



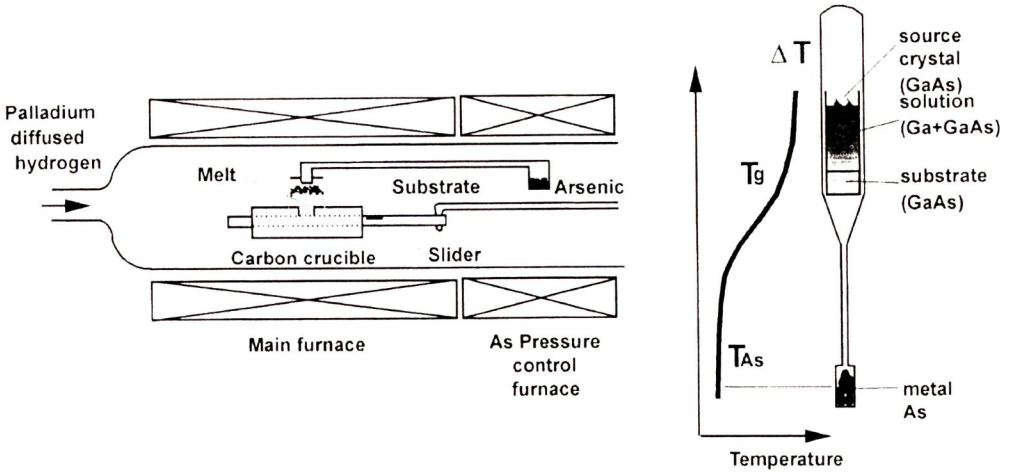


**Fig. 10.** Schematic drawing of the liquid phase epitaxy (LPE) apparatus by the temperature difference method under controlled vapor pressure (TDM-CVP).

made. Driving force for the super-saturation at constant temperature is the difference of solubility and the kinetic energy caused by the temperature difference at the bottom and upper part of the solution. Controlled vapor pressure of group V elements is also applied in order to control the stoichiometric composition of segregated crystals through the Ga-As solution.

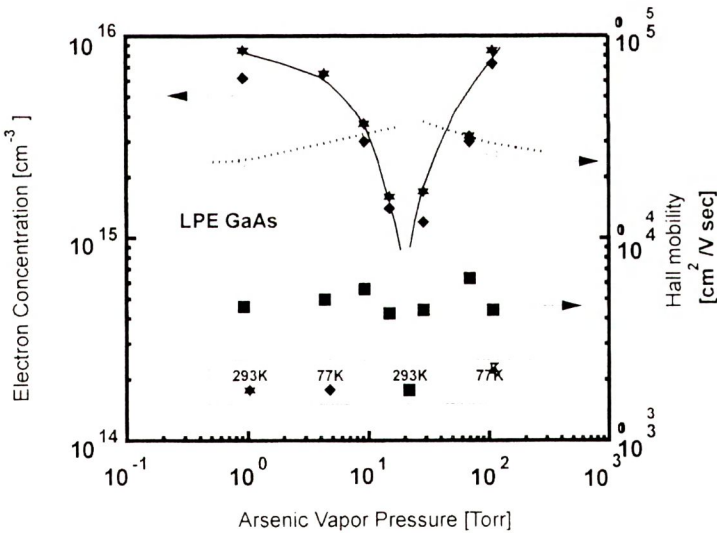


**Fig. 11.** As vapor pressure dependencies of carrier concentration and the electron mobility in LPE GaAs prepared by the TDM-CVP.

Fig. 11 shows the As vapor pressure dependencies of carrier concentration and the electron mobility. Fig. 12 shows the As vapor pressure dependencies of the lattice constant and the half width of the X-ray rocking curve of LPE GaAs. Lattice constant was measured by using GaAs crystal for the first crystal with the (004) symmetric configuration. Therefore, the half width of the

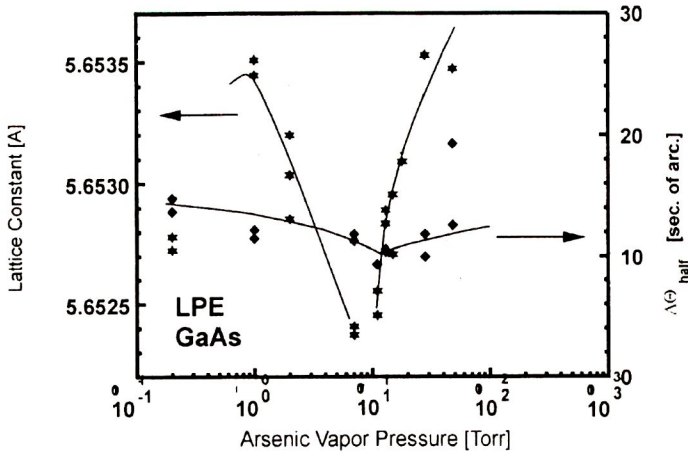


**Fig. 12.** As vapor pressure dependencies of the lattice constant and the half width of the X-ray rocking curve of LPE GaAs.

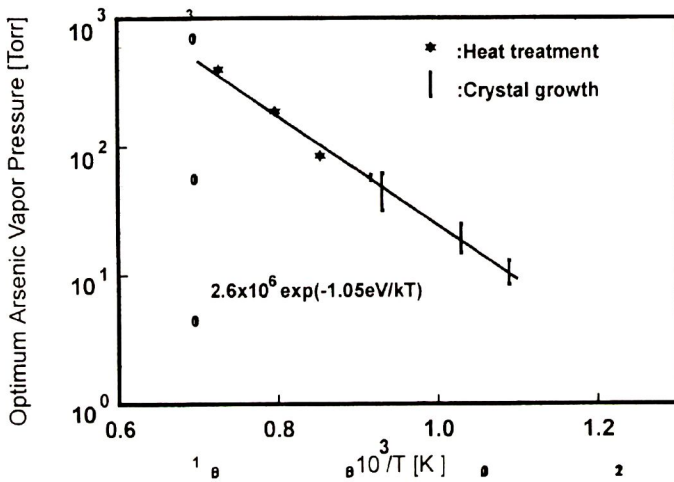


**Fig. 13.** Temperature dependencies of the optimum As vapor pressures obtained from both the LPE growth by TDM-CVP and the annealing experiments under As vapor pressure.

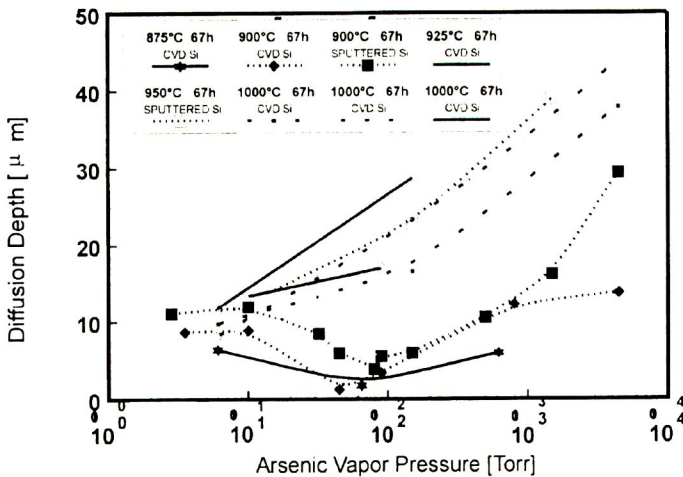


**Fig. 14.** As vapor pressure dependence of the diffusion depth of Si into GaAs from various diffusion source.

X-ray rocking curve is dependent on the perfection of specimen crystals. Under a specific As vapor pressure, carrier concentration shows its minimum value, and the Hall mobility shows maximum. The lattice constant and the half width of X-ray rocking curve also show minimum values under almost the same As vapor pressure. This leads to a crucial conclusion that the high purity LPE crystals with good perfection were obtained. Similar results were also obtained in LPE GaP crystals using TDM-CVP. Especially, photoluminescence (PL) measurements revealed the existence of excitons bound to shallow impurity even at room temperature. This also confirms the high crystal quality of LPE GaP grown by the TDM-CVP [25].

Vapor pressure dependencies of these crystal characteristics seems to be similar to those obtained from the annealing experiments. Fig. 13 shows the temperature dependencies of the optimum As vapor pressures obtained from both the LPE growth by TDM-CVP and the annealing experiments under As vapor pressure [26]. These seems to be similar in both experimental results.

The deviation from the stoichiometric composition of GaAs influences the amphoteric manner of group IV elements in GaAs. As shown in Fig.14, the diffusion phenomenon of Si in GaAs is strongly influenced by the deviation from the stoichiometric composition [27]. Similar results on Si-diffusion into GaAs was also reported by Omura [28].

#### **4. SURFACE TREATMENT BEFORE REGROWTH OF GaAs BY MOLECULAR LAYER EPITAXY (MLE) AND ITS ASSOCIATION WITH THE SURFACE STOICHIOMETRY**

Recent development on semiconductor devices requires extremely thin and multi-layered structures. Nishizawa applied the idea of atomic layer epitaxy (ALE) on the compound semiconductor crystals and realized the monomolecular layer epitaxy of single crystalline GaAs for the first time [29]. ALE was used for the preparation of II-VI compound polycrystalline films by Suntola and coworkers [30]. Second method of his idea based on the chemical reactions of the adsorbates on semiconductor surface. In view of the growth mechanism and the resultant mono-molecular crystal growth, Nishizawa designated this method as the molecular layer epitaxy (MLE). MLE is the promising epitaxial growth method to achieve the precise thickness control with atomic accuracy (AA) and stoichiometric composition.

Fig.15 shows the schematic drawing of the MLE growth apparatus with its growth sequence diagrams of alternate gas injection method. In case of GaAs, source gases typically used for the MLE are triethyl-gallium (TEG), trimethyl-gallium (TMG) for the Ga and  $\text{AsH}_3$  for the arsenic respectively. Precise description for the surface reaction mechanisms in TMG/ $\text{AsH}_3$  system is shown elsewhere [31].

Usually, GaAs crystals are pre-heated just before growth to remove the residual

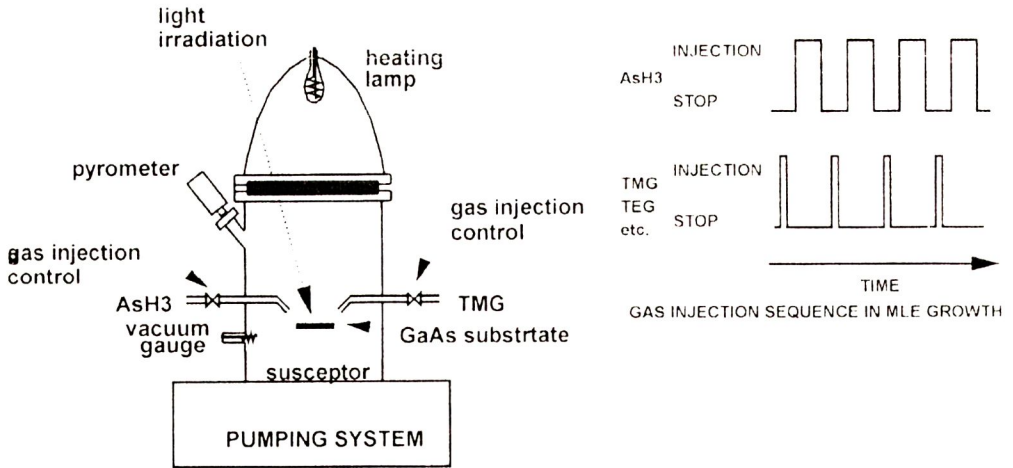


**Fig. 15.** Schematic drawing of the molecular layer epitaxy (MLE) growth apparatus with its growth sequence diagrams of alternate gas injection method.

oxide and/or carbide layer. However, pre-treatment conditions i.e. flush desorption conditions have not been fully optimized yet. This is serious problem to be solved especially in the ultra-thin and multi-layered structures with atomic accuracy.

In order to study the effects of surface treatment procedure and surface stoichiometry on the electrical properties,  $p^+n$  diodes were made by the regrowth on the commercially available MOCVD grown  $n/n^+$ -GaAs epitaxial wafers. Defects at the interfacial region was evaluated by the current-voltage characteristics of regrown  $p^+n$  diodes. Specific forward voltage ( $V_{fs}$ ) at  $1\mu\text{A}$  (pad area is  $100\mu\text{m}^2$ ) is obtained as a function of the various pre-treatment condition for regrowth. Higher  $V_{fs}$  indicates the lower density of recombination center.

Chemical treatments just before MLE is as follows. After degreasing by organic solvent, epitaxial wafers were chemically etched by the sulfuric acid-base etchant with thickness of about  $1500\text{\AA}$ . Then GaAs wafers were dipped in HCl for a few second to reduce the oxide layer thickness. Even after dipping in HCl, XPS (X-ray photo-electron spectroscopy) and Auger electron spectroscopy (AES) analysis revealed the trace of thin oxide layer on the GaAs surface.

Prior to the MLE growth, substrate in the growth chamber was heated to remove the thin oxide layer and to achieve the surface stoichiometry. Growth temperature of MLE used was  $420^\circ\text{C}$ . Mercury lamp was also irradiated on the substrate during growth. DEZn (Di-ethyl-zinc) was used for the  $p$ -type dopant in TEG/AsH<sub>3</sub> system. DEZn injection was done after AsH<sub>3</sub> injection (mode AA) to achieve heavy acceptor doping. Precise description about the doping MLE is shown elsewhere [32]. Regrown structure was  $100\text{\AA}$ -Zn doped  $p^{++}$  top-contact layer with  $p=6 \times 10^{19}\text{cm}^{-3}$ ,  $250\text{\AA}$ -Zn doped  $p^+$  layer with  $p=4 \times 10^{18}\text{cm}^{-3}$  and  $150\text{\AA}$ -none doped layer with  $n < 3 \times 10^{16}\text{cm}^{-3}$ .

These layers were epitaxially regrown on the pre-treated 3500Å thick n-MOCVD grown epitaxial wafers. None-alloyed Ti/Au metal electrode was made on the top p++ contact layer by the conventional lift-off process without any heat treatment. Back contact was formed by the AuGe/Au also without any heat treatment. Current-voltage characteristics were measured at nominal room temperature as the functions of the pre-heating condition of temperature, time and AsH<sub>3</sub> pressure.

Recent XPS and quadru-pole mass spectroscopy (QMS) results show the effect of AsH<sub>3</sub> on the desorption of oxide layer from GaAs surface [33]. In ultra-high vacuum without AsH<sub>3</sub> introduction, Ga oxide layer was desorbed from GaAs surface at around 700°C. Under the existence of AsH<sub>3</sub> ambient, oxide layer can be safely removed at lower temperature. This can be explained by the surface reaction of oxide layer with cracked chemical species of AsH<sub>3</sub>.

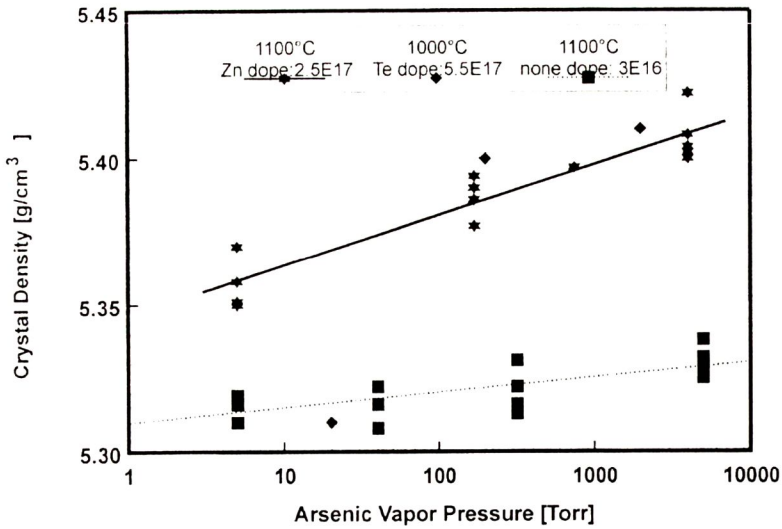
Pre-heating temperature dependence on  $V_{fs}$  shows As shape characteristics. At lower temperature, increase of  $V$  with temperature can be explained due to the removal of residual oxide layer on GaAs. However, at higher temperature, it is considered that surface stoichiometry degrades the I-V characteristics with increasing pre-heating temperature. Pre-heating time and AsH<sub>3</sub> pressure dependencies also confirm these results. Precise results on the flush desorption condition will be shown elsewhere [34].

Stoichiometry control is also quite important factor even in the research field of surface science.

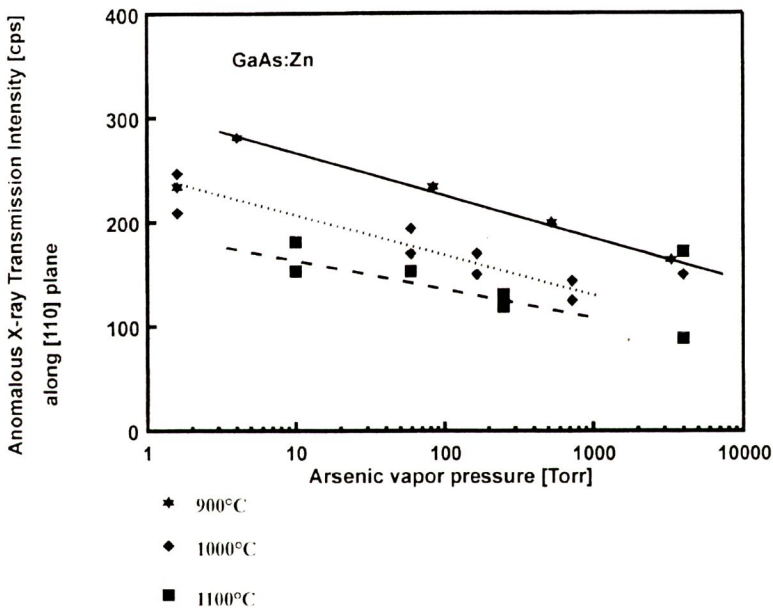
## 5. INTERSTITIAL As ATOMS IN GaAs

Fig. 16 shows the As vapor pressure dependencies of the crystal weight of GaAs prepared by annealing. It is shown that the crystal weight increases monotonically with increasing As vapor pressure. Fig. 17 shows the results of X-ray anomalous transmission intensity measurements as a function of As vapor pressure. The intensity of X-ray anomalous transmission decreases with increasing As vapor pressure. X-ray anomalous transmission is strongly influenced by the existence of interstitial atoms, because this phenomenon is caused by the propagation of Poynting vector of X-ray along the diffracting lattice plane. These results seem to confirm the existence of interstitial type defects when GaAs crystals were annealed under extremely high As vapor pressure.

Fig. 18 shows the As vapor pressure dependence of the lattice constant. Samples used were Zn doped HB grown GaAs prepared by annealing at 900 °C for 67 h under As vapor pressure. As already shown, the lattice constant shows minimum value at the optimum As vapor pressure. In higher As vapor pressure region, the lattice constant increases monotonically with increasing As vapor pressure and shows saturating manner. From the temperature dependence of the saturating lattice constant in high As vapor pressure region, the formation energy of the defect was obtained to be about 0.9 eV.



**Fig. 16.** As vapor pressure dependencies of the crystal weight of GaAs prepared by annealing. Annealing was performed at 900 - 1100° C for 67h.



**Fig. 17.** Change of X-ray anomalous transmission intensity of annealed GaAs as a function of As vapor pressure.

Fig. 19 shows the As vapor pressure dependence of the 1.25 eV level density obtained from the PHCAP measurements. This level is followed by so-called the photoquenching phenomenon. The level density increases monotonically with increase of As vapor pressure, and saturates under high As vapor pressure. From the temperature dependence of the saturating level density, the formation energy of the defect is determined to be 1.16eV (Fig. 20). This formation energy of defect is in

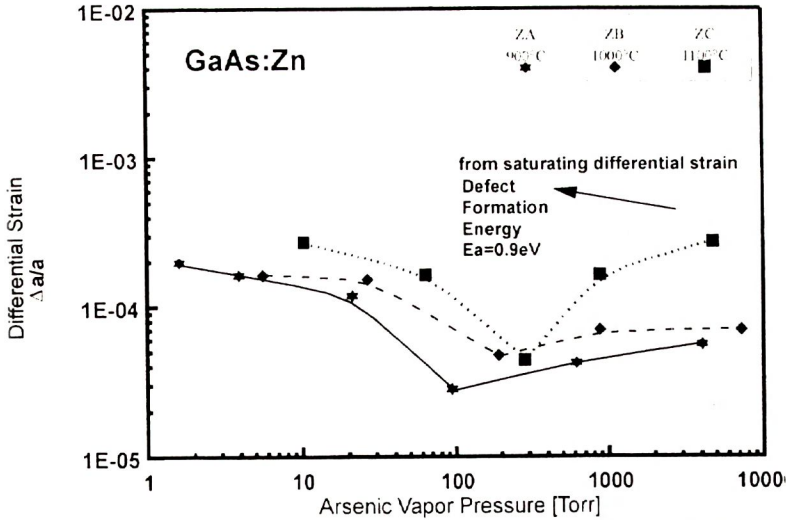


**Fig. 18.** As vapor pressure dependence of the lattice constant of Zn-doped HB grown GaAs prepared by annealing at 900 °C for 67 h.

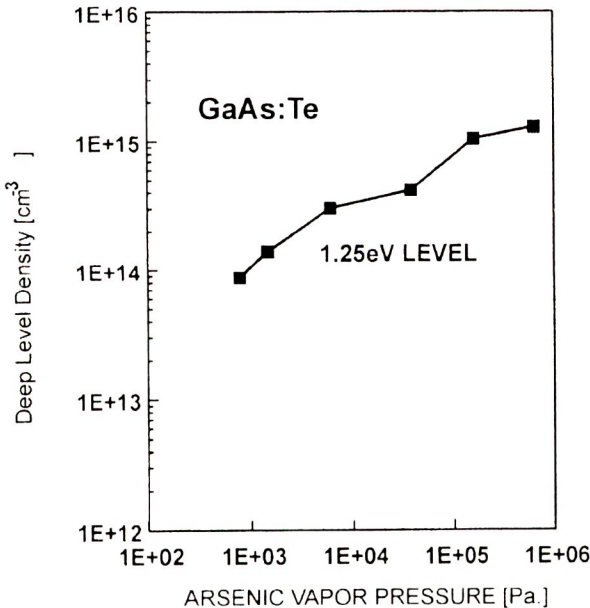


**Fig. 19.** As vapor pressure dependence of the 1.25 eV de-ionized level density obtained from the PHCAP measurements. This level is followed by so-called the photo-quenching phenomenon. Samples used were intentionally-undoped GaAs ( $n=4 \times 10^{16} \text{cm}^{-3}$ ) grown by HB method.

good accordance with that obtained from the lattice constant measurements.

From the theoretical calculations of formation energy by K.H. Bennemann [35] and R.A. Swalin [36], the defect formation energy of 1.16 eV is rather close to that of interstitial atoms than that of vacancy. Therefore, we consider

that the interstitial atoms should be introduced at the primary stage of defect formation when GaAs was annealed under high As vapor pressure.

In order to investigate the stable interstitial site, we applied the RBS technique to the As<sup>+</sup> implanted GaAs crystals. Depth resolution was enhanced by using the grazing exit angle configuration of silicon surface barrier (SSB) detector. From the results of multi-directional and high depth resolution RBS measurements, the stable interstitial site was assumed to be <100> split and relaxed bond center (r-BC) interstitialcy. This RBS result corresponds to that obtained from the X-ray anomalous transmission measurements.

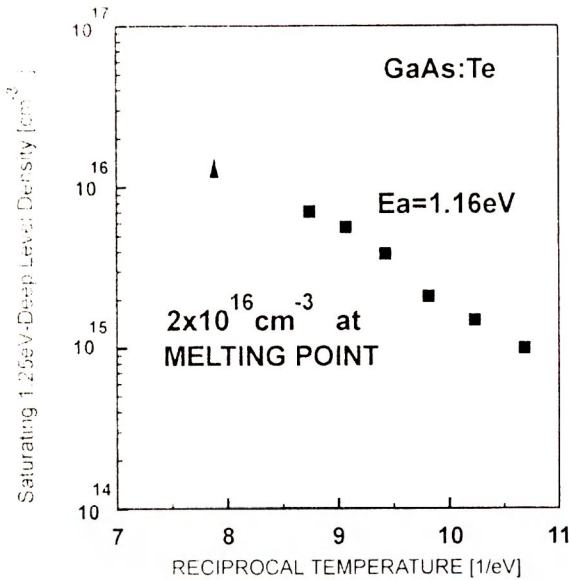


**Fig. 20.** Annealing temperature dependence (Arrhenius plot) of the 1.25 eV level density in *n*-GaAs saturated under high As vapor pressure.

## 6. GaAs BULK CRYSTAL GROWTH BY THE VAPOR PRESSURE CONTROLLED CZOCHRALSKI (PCZ) METHOD

Vapor pressure control technology established by our annealing and LPE experiments under controlled vapor pressure is also extended into the GaAs bulk crystal melt growth. The vapor pressure control of the GaAs solution growth was carried out at first by T.Suzuki and S.Akai [37] in the field of the horizontal Bridgman (HB) method. High quality GaAs bulk crystals with very low dislocation density were grown under our finding optimum As vapor pressure of 830 Torr, where the temperature of metal As is 617°C. These crystals are now supplied all over the world. Thereafter, this work was also reconfirmed by Gatos and Nanishi [38], and it was shown that the dislocation density and the defect density decreased abruptly at a specific metal As temperature of 617°C within 1°C. This specific As vapor pressure is nearly equal to that obtained from our equation (2) concerning on the temperature dependence of the optimum As vapor pressure. Optimum As vapor pressure at melting point of GaAs is obtained to be 830 Torr from the eqn. (2) The temperature of the metal As corresponds to be 617°C according to the eqn. (1).

Whereas the dislocation density has been greater than that of HB crystals due to its large thermal strain, conventional CZ method enables the growth of GaAs bulk crystals with large diameter compared with the HB method. By applying the vapor pressure control method to the CZ growth (PCZ), high quality CZ GaAs bulk crystals with very low dislocation density were obtained. As shown in Fig. 21, 2-inch wafers with the



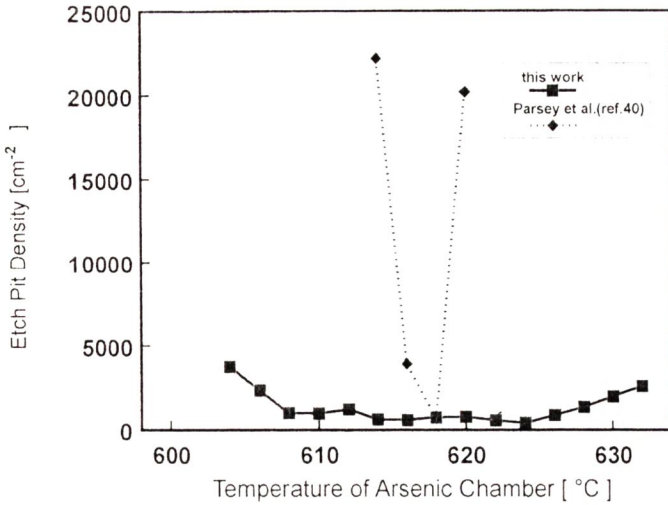


**Fig. 21.** Spatial distribution of etch pit density across the PCZ grown GaAs bulk crystal. Dislocation etch pits were revealed by the molten KOH etchant.

dislocation density as low as  $500 \text{ cm}^{-2}$  were grown without impurity doping under the optimum As vapor pressure. The etch pit density (EPD) of the intentionally undoped LEC GaAs is about  $10^5 \text{ cm}^{-2}$ . This is higher at least one order of magnitude than that of PCZ grown GaAs crystals. DLTS measurements revealed three kinds of deep donors. Fig. 22 shows the As vapor pressure dependence of each deep level density. It is shown that the deep level

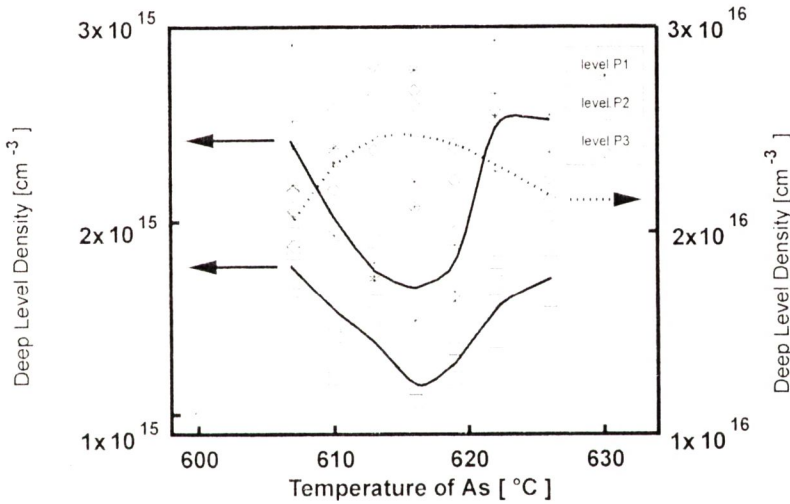


**Fig. 22.** As vapor pressure dependence of the deep level density of PCZ grown GaAs bulk crystals revealed by deep level transient spectroscopy (DLTS).

density also shows minimum under optimum As vapor pressure. Similar results were also obtained from the PHCAP measurements. Fig. 23 shows the photographs of the PCZ and conventional CZ grown GaAs ingots. Surface of the PCZ GaAs crystals is shown to be very brilliant compared to that of the conventional LEC crystals.

In order to evaluate deep levels in various GaAs bulk crystals, the PHCAP measurements were carried out under constant capacitance condition. Fig. 24 shows

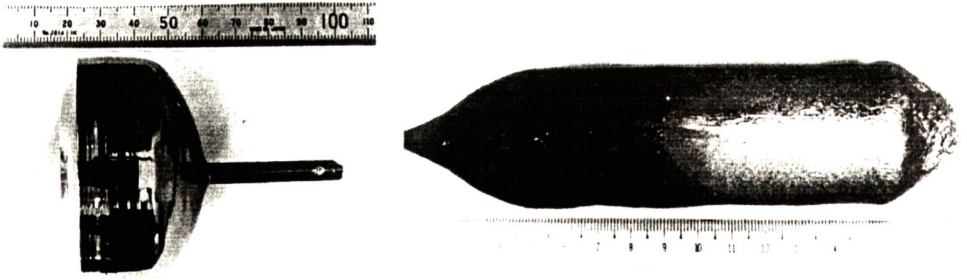


Fig. 23. Photographs of the as-grown surface of PCZ and conventional CZ grown GaAs in-

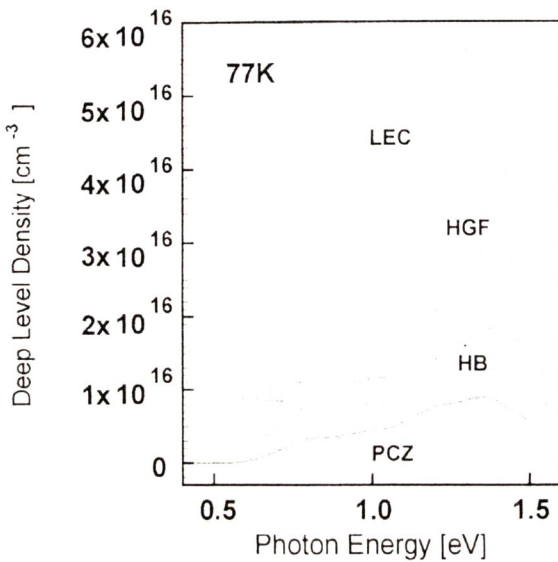


Fig. 24. Ion density PHCAP spectra of various intentionally-undoped  $n$ -GaAs crystals with the carrier concentration of about  $4 \times 10^{16} \text{ cm}^{-3}$ .

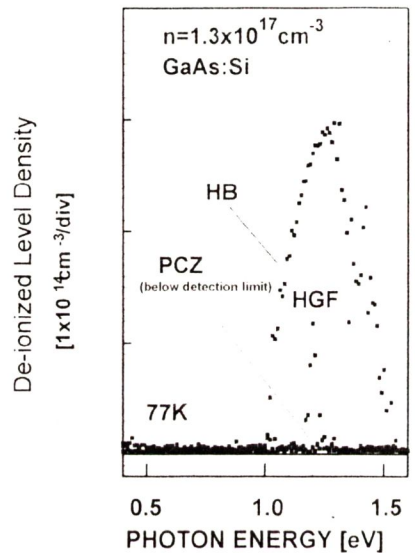


Fig. 25. As vapor pressure dependencies of the lattice constant and the half width of the X-ray rocking curve of LPE GaAs.

the PHCAP spectra of various intentionally-undoped  $n$ -GaAs crystals with the carrier concentration of about  $4 \times 10^{16} \text{ cm}^{-3}$ . As reported previously, the so-called photoquenching phenomenon is observed in the spectral region of 1.0 -1.50 eV below about 110 K. After irradiation of monochromatic light, ion density increases rapidly and then decreases gradually. PCZ crystal shows minimum deep level density compared with that of other crystals. This confirms the possibility for perfect crystal growth by the PCZ method. Fig. 25 shows the PHCAP spectra obtained from the subtraction between maximum and saturating ion density at each wavelength. Samples used were

various Si-doped GaAs bulk crystals with the carrier concentration of  $1.5 \times 10^{17} \text{ cm}^{-3}$  grown by various methods. PCZ crystal shows extremely low deep level density, which shows the so-called photoquenching phenomenon.

## 7. GaAs BULK CRYSTAL GROWN BY THE VAPOR PRESSURE CONTROLLED FZ (VPC-FZ) METHOD

In order to obtain high purity bulk crystals with stoichiometric composition, vapor pressure controlled FZ method (VPC-FZ) has been applied to GaAs bulk crystal growth [39, 40]. FZ method has the possibility to minimize the unintentional impurity contamination from crucible. Whereas the growth condition has not been optimized and the As vapor pressure is not strictly controlled yet, high purity *p*-GaAs crystals were obtained with the carrier concentration as low as about  $1 \times 10^{15} \text{ cm}^{-3}$ . Fig. 26 shows the PHCAP spectrum of the VPC-FZ grown *p*-GaAs crystal. Stoichiometry-dependent deep acceptors were detected at 0.53, 0.71, 0.90 and 1.0 eV above the valence band. These deep levels were commonly detected regardless of the variation

of dopant impurities and growth method. As vapor pressure dependencies of the level density were also clarified by out PHCAP measurements.

However, the level density in VPC-FZ GaAs is much lower than that in LEC and HB grown samples by three order in magnitude. This confirms the ability of VPC-FZ method to supply high purity GaAs crystals with stoichiometric composition.

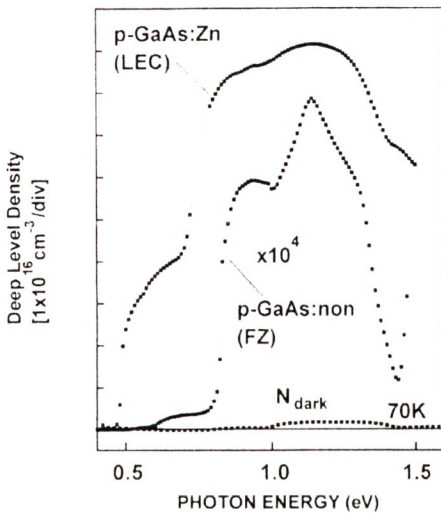


**Fig. 26.** Ion density PHCAP spectrum of the vapor pressure controlled FZ (VPC-FZ) grown *p*-GaAs crystal. *p*-GaAs crystals were obtained with the carrier concentration as low as about  $1 \times 10^{15} \text{ cm}^{-3}$ .

### EDITORIAL NOTE

The paper submitted by the authors was divided by the editor into three parts which will be successively published. Part one, published above discusses stoichiometry - dependent deep centres in GaAs. Part two and part three will be published in the next issues of "Materiały Elektroniczne" dedicated to deep levels related to stoichiometry of InP and AlGaAs, respectively.

## REFERENCES

- [1] Watanabe Y., Nishizawa J., Sunagawa I.: *Kagaku* 121, 3, 140-141, Iwanami 1951
- [2] Otsuka H., Ishida K., Nishizawa J. *Jpn. J. Appl. Phys.* 8, 1969, 632
- [3] Nishizawa J., Shinozaki S. Ishida K.: *J. Appl. Phys.* 14, 1974, 1638
- [4] Nishizawa J., Otsuka H., Yamakoshi S., Ishida K.: *Jpn. J. Appl. Phys.* 13, 1974, 46
- [5] Yamakoshi S., Doctor Thesis, Tohoku University 1975 supervised by prof. Nishizawa
- [6] Nishizawa J., Shiota I., Oyama Y.: *J. Phys. C: Solid State Phys.* 9, 1986, 1
- [7] Nishizawa J., Oyama Y., Dezaki K.: *J. Appl. Phys.* 67(4) 1990, 1884
- [8] Nishizawa J., Oyama Y., Dezaki K.: *Phys. Rev. Lett.* 65, 1990, 2555
- [9] Fujimoto I.: *Jpn. J. Appl. Phys.*, 23, 1984, L287
- [10] Nishizawa I., Ito K., Okuno Y., Sakurai F., Koike M., Teshima T.: *Proceedings of the IEEE International Electron Device Meeting*, 1983, 311-314
- [11] Nishizawa J., Itoh K., Okuno Y., Koike M., Teshima T.: *Proc. IEEE International Electron Devices Meeting (IEDM)* 1983, 311-314
- [12] Nishizawa J., Okuno Y., Koike M., Sakurai F.: *Jpn. J. Appl. Phys.* 19, 1980, 377
- [13] Nishizawa J., Shinozaki S., Ishida, K.: *J. Appl. Phys.* 14, 1974, 1638
- [14] Nishizawa J., Inokuchi K.: *Proc. in International Optoelectronics Workshop*, Taiwan, 1981
- [15] Suzuki T., Akai S.: *Bussei* 12, 1971, 144
- [16] Parsey M., Jr., Nanishi Y., Lagowski J. Gatos H.C.: *J. Electrochem. Soc.* 128, 1981, 937
- [17] Honig R.E.: *RCA Rev.* 30, 1969, 285
- [18] Itoh A., Sukegawa T., Nishizawa, J.: *Tech. Report of Transistor Specialist Committee, IEE Japan* (Jan.1967), Itoh A., Sukegawa T., Nishizawa J.: *Tech. Report of Research Institute of Electrical Communication, Tohoku University*, TR-32 (Feb.1969)
- [19] Oyama Y.: *Denshi Tokyo (IEEE Tokyo)*, 28, 1989, 130
- [20] Lin A.L., Omelianovski E., Bube R.H.: *J. Appl. Phys.* 47, 1976, 1852
- [21] Nishizawa J., Oyama Y., Dezaki K.: *J. Appl. Phys.* 67(4), 1990, 1884
- [22] Nishizawa J., Oyama Y., Dezaki K.: *J. Appl. Phys.* 69(3), 1991, 1446
- [23] Nishizawa J., Oyama Y., Dezaki K.: *J. Phys. Condensed Matter* 3, 1991, 7269
- [24] Nishizawa J., Oyama Y., Dezaki K.: *J. Appl. Phys.* 70(2), 1991, 833
- [25] Suto K., Nishizawa J.: *J. Appl. Phys.* 67(1), 1990, 459
- [26] Nishizawa J., Okuno Y.: *Proc. of 2nd International School on Semiconductor Optoelectronics*, Cetniewo, ed. by M.A. Herman, Warszawa, PWN-Polish Scientific Publishers, 1978, 101-130
- [27] Kobayashi Y., Okuno Y., Nishizawa J.: *RIEC (Research Institute of Electrical Communication, Tohoku University) Technical Report*, TR-42, 1978
- [28] Omura E., Wu X.X., Vawter G.A., Coldren L., Hu E., Merz J.L.: *Electron. Lett.* 22, 1986, 496

- [29] Nishizawa J., Abe H., Kurabayashi T.: J. Electrochem. Soc. 132 1983, 1197
- [30] Ahonen M., Pessa M., Suntla T.: Thin Solid Films 65, 1980, 301
- [31] Nishizawa J., Sakuraba H., Oyama Y.: Thin Solid Films 225, 1993, 1
- [32] Nishizawa J., Abe H., Kurabayashi T.: J. Electrochem. Soc. 36(2), 1989, 478
- [33] Oyama Y., Plotka P., Nishizawa J.: Applied Surface Science 82/83,1994, 41
- [34] Nishizawa J., Oyama Y., Plotka P., Sakuraba H.: Surface Science 348, 1996, 105-114
- [35] Bennemann K.H.: Phys. Rev.137, 1961, AI 497
- [36] Swalin R.A.: J. Phys. Chem. Solids 18, 1961, 290
- [37] Suzuki T., Akai S.: Bussei 144, 1971, 12
- [38] Parsey J.M. Jr, Nanishi Y., Lagowski L., Gatos H.C.: J. Electrochem. Soc. 128, 1981,937
- [39] FZ grown GaAs crystals were supplied from the Tohoku Steel Co'Ltd, Sendai Japan
- [40] Lang D.V., Rogan R.A., Jaros M.: Phys.Rev. B19, 1979 1015  
Chadi D.J., Chang K.J.: Phys.Rev. B 39,14, 1989, 10063  
Mooney P.M.: J.Appl.Phys. 67, 3, 1990, R1  
Dmochowski J.E., Dobaczewski L., Langer J.M.: Wolfgang Jantsch Phys.Rev.B 40,14, 1989, 9671  
Cheong B.H., Chang K.J.: Phys.Rev.B 46, 20, 1992, 13131